

## Base-Induced Dismutation of POCl<sub>3</sub> and POBr<sub>3</sub>: Synthesis and Structure of Ligand-Stabilized Dioxophosphonium Cations

Pavel Rovnaník, Libor Kapička, Jan Taraba, and Miloš Černík\*

Department of Inorganic Chemistry, Masaryk University, Kotlarska 2,  
611 37 Brno, Czech Republic

Received December 10, 2003

The interaction between POCl<sub>3</sub> or POBr<sub>3</sub> and pyridine or DMAP has been reinvestigated to clarify the discrepancies between previously published results concerning the Lewis acidity of phosphoryl halides and their behavior toward pyridine bases. The obtained results show that POCl<sub>3</sub> virtually does not react with pyridine, while it does with 4-(dimethylamino)pyridine (DMAP), even in SO<sub>2</sub> solution, to yield an ionic compound [(DMAP)<sub>2</sub>PO<sub>2</sub>]Cl·3SO<sub>2</sub> (**1**·3SO<sub>2</sub>). Its recrystallization from acetonitrile gives [(DMAP)<sub>2</sub>PO<sub>2</sub>]Cl·CH<sub>3</sub>CN (**1**·CH<sub>3</sub>CN). The POBr<sub>3</sub> reacts readily with both DMAP and pyridine forming the analogous tribromides, [(DMAP)<sub>2</sub>PO<sub>2</sub>]Br<sub>3</sub> (**2**) and [(py)<sub>2</sub>PO<sub>2</sub>]Br<sub>3</sub> (**3**), respectively. Treatment of **3** with Me<sub>3</sub>SiOSO<sub>2</sub>CF<sub>3</sub> in acetonitrile solution led to [(py)<sub>2</sub>PO<sub>2</sub>][CF<sub>3</sub>SO<sub>3</sub>]·CH<sub>3</sub>CN (**4**), while the reaction between **1**·CH<sub>3</sub>CN and Me<sub>3</sub>SiOPOF<sub>2</sub> gave [(DMAP)<sub>2</sub>PO<sub>2</sub>][PO<sub>2</sub>F<sub>2</sub>] (**5**). The crystal structures of **1**·CH<sub>3</sub>CN, **1**·3SO<sub>2</sub>, **2**, and **4** revealed that all four compounds are ionic containing the distorted tetrahedral cations [(DMAP)<sub>2</sub>PO<sub>2</sub>]<sup>+</sup> and [(py)<sub>2</sub>PO<sub>2</sub>]<sup>+</sup>. Both ions represent a donor-stabilized form of the so far unknown cation [PO<sub>2</sub>]<sup>+</sup>. The geometry of [(DMAP)<sub>2</sub>PO<sub>2</sub>]<sup>+</sup>, optimized by density functional calculations at the B3LYP/6-31G(d,p) level, is in good agreement with X-ray structural data. The NBO analysis of natural atomic charges shows an extensive delocalization of the [PO<sub>2</sub>]<sup>+</sup> intrinsic positive charge and indicates a contribution of the electrostatic attraction to the formation of N–P donor–acceptor bonds. According to a <sup>31</sup>P NMR study, the reactions of both phosphoryl halides with DMAP proceed via successive formation of the intermediates [(DMAP)POX<sub>2</sub>]<sup>+</sup> and (DMAP)PO<sub>2</sub>X to give an equimolar mixture of [(DMAP)<sub>2</sub>PO<sub>2</sub>]<sup>+</sup> and PX<sub>5</sub> (X = Cl, Br) as the end products. The NMR spectroscopic identification of the cations [(DMAP)POX<sub>2</sub>]<sup>+</sup> and [(DMAP)<sub>2</sub>PO<sub>2</sub>]<sup>+</sup> was supported by ab initio calculations of their chemical shifts.

### Introduction

The oxygen atom in phosphoryl chloride may act as an electron-pair donor toward strong Lewis acids, and the formation of numerous oxygen-bridged complexes between metal or metalloid halides and POCl<sub>3</sub> has been reported. Most of them are simple covalent adducts of the type Cl<sub>3</sub>PO-(MHal<sub>n</sub>),<sup>1</sup> but ionic structures have been proposed for some complexes formed with AlCl<sub>3</sub><sup>2</sup> and FeCl<sub>3</sub>.<sup>1</sup> However, literature evidence about the POCl<sub>3</sub> ability to form adducts

with Lewis bases is scarce and contradictory, and the structures of the described compounds are unknown. An earlier study of the phase diagram of the pyridine–POCl<sub>3</sub> binary system showed an absence of the formation of any addition compound, if rigorously dried POCl<sub>3</sub> and pyridine were used.<sup>3</sup> On the other hand, adducts, such as POCl<sub>3</sub>(py)<sub>2</sub>,<sup>4</sup> POCl<sub>3</sub>(py)<sub>3</sub>, POCl<sub>3</sub>(4-picoline)<sub>3</sub>, and POCl<sub>3</sub>(quinoline)<sub>3</sub>,<sup>5</sup> were later isolated and characterized by elemental analysis and infrared spectroscopy. It was also reported that DMAP reacts with POCl<sub>3</sub> to produce a solid 3:1 adduct with a proposed ionic structure of tris(onio)-substituted phosphoryl chloride, [(DMAP)<sub>3</sub>PO]Cl<sub>3</sub>.<sup>6</sup> Its low solubility, however, did not permit

\* Author to whom correspondence should be addressed. E-mail: cernik@chemi.muni.cz. Fax: +420-5-41211214.

(1) (a) Burford, N.; Phillips, A. D.; Schurko, R. W.; Wasylishen, R. E.; Richardson, J. F. *Chem. Commun.* **1997**, 2363. (b) Boghosian, S.; Voyiatzis, G. A.; Papatheodorou, G. N. *J. Chem. Soc., Dalton Trans.* **1996**, 3405. (c) Petersen, J.; Lork, E.; Mews, R. *Chem. Commun.* **1996**, 1897. (d) Klingelhöfer, P.; Müller, U.; Hauck, H. G.; Dehnicke, K. Z. *Naturforsch., B* **1984**, 39, 135 and references therein.  
(2) Birkeneder, F.; Berg, R. W.; Bjerrum, N. J. *Acta Chem. Scand.* **1993**, 47, 344.

(3) Zeffert, B. M.; Coulter, P. B.; Macy, R. *J. Am. Chem. Soc.* **1953**, 75, 751.

(4) Gutmann, V. *Monatsh. Chem.* **1954**, 85, 1077.

(5) Paul, R. C.; Khurana, H.; Vasisht, S. K.; Chadha, S. L. *J. Indian Chem. Soc.* **1969**, 46, 915.

(6) Weiss, R.; Engel, S. *Synthesis* **1991**, 10, 1077.

one to record the  $^{31}\text{P}$  NMR spectrum or to grow single crystals for an X-ray structure determination, and thus, a reliable structural assignment of this compound is not yet available.

Analogous complexes of  $\text{POBr}_3$  were even less frequently studied. Covalent 1:1, 1:2, or 1:3 molecular adducts of  $\text{POBr}_3$  with metal bromides or chlorides<sup>7</sup> have been described, while 1:3 or 1:4 donor–acceptor complexes are allegedly formed with pyridine, 4-picoline, quinoline, and piperidine.<sup>5</sup>

In contrast to  $\text{POCl}_3$ , the isovalent  $\text{SiCl}_4$  exhibits distinct properties of a Lewis acid and with suitable bases forms neutral adducts, e.g.  $\text{SiCl}_4(\text{py})_2$ ,<sup>8</sup> as well as cationic complexes with a ligand-stabilized  $[\text{SiCl}_2]^{2+}$  dication, e.g.  $[\text{SiCl}_2(\text{NMI})_4]^{2+}$  (NMI = *N*-methylimidazole).<sup>9</sup> In both types of compounds the central silicon is six-coordinated with chlorine atoms and unidentate nitrogen bases, showing a slightly distorted octahedral geometry. To clarify the differences between chemical reactivities of  $\text{POCl}_3$  and  $\text{SiCl}_4$  toward Lewis bases and to elucidate the nature of the resulting complexes, reactions of  $\text{POCl}_3$  with pyridine and DMAP have been reexamined and a parallel study with  $\text{POBr}_3$  has been performed to enable a comparison with  $\text{POCl}_3$ .

## Experimental Section

**Materials and Apparatus.** All reactions and manipulations of air-sensitive reagents were carried out under strictly anhydrous conditions using standard grease-free glass vacuum line and Schlenk techniques. Solvents and pyridine were dried over  $\text{P}_4\text{O}_{10}$ , distilled from  $\text{CaH}_2$ , and stored over activated molecular sieves. DMAP was dried over 4 Å molecular sieve and sublimed in vacuo. Phosphorus oxide chloride (Riedel-de Haën) was crystallized twice at 0–0.5 °C, i.e., slightly under its freezing point, and distilled. Phosphorus oxide bromide was prepared by following the published procedure<sup>10</sup> and sublimed under vacuum.  $\text{Me}_3\text{SiOSO}_2\text{CF}_3$  (Aldrich) was used without further purification.  $\text{Me}_3\text{SiOP}(\text{O})\text{F}_2$  was prepared by the reaction of hexamethyldisiloxane with  $\text{POF}_3$  at room temperature and fractionated under vacuum.<sup>11</sup> Gravimetric chemical analysis was carried out for halogens and phosphorus. The fluoride was determined as  $\text{PbBrF}$  after steam distillation,<sup>12</sup> chloride and bromide were determined as  $\text{AgCl}$  and  $\text{AgBr}$ , respectively, and phosphorus was determined as quinolinium phosphomolybdate.<sup>13</sup> The pyridines were distilled off from concentrated alkaline solutions and determined acidimetrically. The  $^1\text{H}$ ,  $^{19}\text{F}$ , and  $^{31}\text{P}$  NMR spectra were recorded on a Bruker Avance DPX 300 spectrometer using a 5 mm multinuclear QNP probe head and operating at 300.00, 282.40, and 121.49 MHz, respectively. Chemical shifts, in ppm, are referenced relative to external standards  $\text{Me}_4\text{Si}$  ( $^1\text{H}$ ),  $\text{CFCl}_3$  ( $^{19}\text{F}$ ), and 85%  $\text{H}_3\text{PO}_4$  ( $^{31}\text{P}$ ) with negative shifts being upfield from the reference signal.  $\text{D}_2\text{O}$  was used as an external  $^2\text{H}$  lock.

**Preparation of  $[(\text{DMAP})_2\text{PO}_2]\text{Cl}\cdot 3\text{SO}_2$  (**1**· $3\text{SO}_2$ ).** In a typical procedure, DMAP (1.55 g, 12.7 mmol) was dissolved in liquid  $\text{SO}_2$  (6.55 g) in a two-bulbed reaction vessel with an integral sintered-glass filter and two Rotaflo valves.  $\text{POCl}_3$  (1.98 g, 12.9 mmol) was condensed onto the frozen solution at  $-196$  °C. Upon warming of the sample to room temperature and mixing, the vessel was allowed to stand at 20 °C for 7 days. Thereafter, ca. 80% of the solvent (5.11 g) was distilled off at  $-30$  °C and the vessel was left overnight at ambient temperature. The deposited colorless crystals of **1**· $3\text{SO}_2$  were filtered off and dried shortly under vacuum. At reduced pressure, however, the crystals disintegrated readily evolving  $\text{SO}_2$  even at  $-10$  °C, and chemical analysis revealed that their composition depended upon the length of pumping. The formula **1**· $3\text{SO}_2$  is therefore derived from the results of X-ray structure analysis. Yield: 2.27 g (67%).  $^1\text{H}$  NMR ( $\text{SO}_2$ ):  $\delta$  4.35 (s, 12H), 7.94 (d, 4H), 9.34 (d, 4H).  $^{31}\text{P}$  NMR ( $\text{SO}_2$ ):  $\delta$   $-13.7$  (s).

**Preparation of  $[(\text{DMAP})_2\text{PO}_2]\text{Cl}\cdot\text{CH}_3\text{CN}$  (**1**· $\text{CH}_3\text{CN}$ ).** The recrystallization of **1**· $3\text{SO}_2$  (1.92 g) from hot acetonitrile (70 °C) gave colorless crystals of **1**· $\text{CH}_3\text{CN}$ . Yield: 1.14 g (83%).  $^1\text{H}$  NMR ( $\text{SO}_2$ ):  $\delta$  4.35 (s, 12H), 7.94 (d, 4H), 9.34 (d, 4H).  $^{31}\text{P}$  NMR ( $\text{SO}_2$ ):  $\delta$   $-13.7$  (s). Mp: 246 °C. Anal. Calcd for  $\text{C}_{16}\text{H}_{22}\text{ClN}_5\text{O}_2\text{P}$ : Cl, 9.24; N(pyridinic), 7.30; P, 8.07. Found: Cl, 9.39; N(pyridinic), 7.93; P, 8.15.

**Preparation of  $[(\text{DMAP})_2\text{PO}_2][\text{Br}_3]$  (**2**).** The mixture of **3** (2.64 g, 5.6 mmol) and DMAP (1.54 g, 12.66 mmol) was dissolved in liquid  $\text{SO}_2$  (9.51 g) to give a brown solution, which was allowed to stand at room temperature for 1 h. The volatile materials were removed in vacuo to leave a brown solid. The crude product was recrystallized from hot  $\text{CH}_3\text{CN}$ , filtered off, and vacuum-dried. Yield: 2.25 g (72%).  $^1\text{H}$  NMR ( $\text{SO}_2$ ):  $\delta$  4.23 (s, 12H), 7.90 (d, 4H), 9.21 (d, 4H).  $^{31}\text{P}$  NMR ( $\text{SO}_2$ ):  $\delta$   $-13.7$  (s). Mp: 217–218 °C (dec). Anal. Calcd for  $\text{C}_{14}\text{H}_{20}\text{Br}_3\text{N}_4\text{O}_2\text{P}$ : Br, 43.82; N(pyridinic), 5.12; P, 5.66. Found: Br, 44.03; N(pyridinic), 5.56; P, 5.49.

**Preparation of  $[(\text{py})_2\text{PO}_2][\text{Br}_3]$  (**3**).** An excess of pyridine (1.5 mL, 22.9 mmol) was added dropwise to the stirred solution of  $\text{POBr}_3$  (4.50 g, 15.6 mmol) in  $\text{CH}_3\text{CN}$  (14 mL) at 0 °C. The resulting yellow solution was allowed to warm to room temperature and stand for 2 days. The precipitated pale yellow, microcrystalline solid was separated by filtration, washed with  $\text{CH}_2\text{Cl}_2$ , and dried in vacuo. Attempts to obtain single crystals suitable for X-ray structure determination were not successful. Yield: 6.21 g (86%).  $^1\text{H}$  NMR ( $\text{SO}_2$ ):  $\delta$  9.36 (d, 4H), 9.86 (t, 2H), 10.43 (d, 4H).  $^{31}\text{P}$  NMR ( $\text{SO}_2$ ):  $\delta$   $-14.2$  (s). Mp: 163–164 °C (dec). Anal. Calcd for  $\text{C}_{10}\text{H}_{10}\text{Br}_3\text{N}_2\text{O}_2\text{P}$ : Br, 52.01; N(pyridinic), 6.08; P, 6.72. Found: Br, 52.56; N(pyridinic), 5.84; P, 6.67.

**Preparation of  $[(\text{py})_2\text{PO}_2][\text{CF}_3\text{SO}_3]\cdot\text{CH}_3\text{CN}$  (**4**).** Liquid  $\text{Me}_3\text{SiOSO}_2\text{CF}_3$  (0.196 g, 0.88 mmol) was added to a solution of **3** (0.204 g, 0.44 mmol) in  $\text{CH}_3\text{CN}$  (3 mL) and stirred for 1 h at room temperature. The solution was evaporated to half of the original volume and slowly cooled to 0 °C to give colorless crystals of **4** suitable for X-ray diffraction study. Yield: 0.114 g (64%).  $^{19}\text{F}$  NMR ( $\text{CH}_3\text{CN}$ ):  $\delta$   $-78.9$  (s).  $^{31}\text{P}$  NMR ( $\text{CH}_3\text{CN}$ ):  $\delta$   $-14.6$  (s).

**Preparation of  $[(\text{DMAP})_2\text{PO}_2][\text{PO}_2\text{F}_2]$  (**5**).** **1**· $\text{CH}_3\text{CN}$  (0.32 g, 0.93 mmol) was added to a solution of  $\text{Me}_3\text{SiOP}(\text{O})\text{F}_2$  (0.19 g, 1.10 mmol) in  $\text{CH}_3\text{CN}$  (17 mL). The mixture was heated to 80 °C for 2 h, until all the solid dissolved. A white solid that precipitated upon cooling to ambient temperature was filtered off and vacuum-dried. Yield: 0.290 g (77%).  $^{19}\text{F}$  NMR ( $\text{CH}_3\text{CN}$ ):  $\delta$   $-82.1$  (d,  $^1J_{\text{PF}} = 949$  Hz).  $^{31}\text{P}$  NMR ( $\text{CH}_3\text{CN}$ ):  $\delta$   $-12.6$  (t,  $^1J_{\text{PF}} = 949$  Hz),  $-13.7$  (s). Anal. Calcd for  $\text{C}_{14}\text{H}_{20}\text{F}_2\text{N}_4\text{O}_4\text{P}_2$ : F, 9.31; N(pyridinic), 6.86; P, 15.17. Found: F, 8.93; N(pyridinic), 7.15; P, 15.08.

**X-ray Structure Determinations for **1**· $3\text{SO}_2$ , **1**· $\text{CH}_3\text{CN}$ , **2**, and **4**.** The intensity data of **1**· $3\text{SO}_2$ , **1**· $\text{CH}_3\text{CN}$ , **2**, and **4** were collected

- (7) (a) Wartenberg, E. W.; Goubeau, J. *Z. Anorg. Allg. Chem.* **1964**, 329, 269. (b) van der Veer, W.; Jellinek, F. *Recl. Trav. Chim.* **1970**, 89, 833. (c) Okuda, T.; Ishihara, H.; Yamada, K.; Negita, H. *Bull. Chem. Soc. Jpn.* **1978**, 51, 1273 and references therein.  
 (8) Bechstein, O.; Ziemer, B.; Hass, D.; Trojanov, S. I.; Rybakov, V. B.; Maso, G. N. *Z. Anorg. Allg. Chem.* **1990**, 582, 211.  
 (9) Hensen, K.; Mayr-Stein, R.; Stumpf, T.; Pickel, P.; Bolte, M.; Fleischer, H. *J. Chem. Soc., Dalton Trans.* **2000**, 473.  
 (10) Gerrard, W.; Nechvatal, A.; Wyvill, P. L. *Chem. Ind.* **1947**, 437.  
 (11) Cavell, R. G.; Leary, R. D.; Tomlinson, A. J. *Inorg. Chem.* **1972**, 11, 2573.  
 (12) Pietzka, G.; Ehrlich, P. *Angew. Chem.* **1953**, 65, 131.  
 (13) Dahlgren, S. E. *Z. Anal. Chem.* **1962**, 189, 243.

on a KUMA KM-4 CCD  $\kappa$ -axis diffractometer equipped with an Oxford Cryosystem LT-device using graphite monochromatized Mo  $K\alpha$  radiation ( $\lambda = 0.71069 \text{ \AA}$ ). The data sets were collected at  $-153 \text{ }^\circ\text{C}$  and corrected for absorption effects using  $\psi$ -scans. The structures were solved by direct methods. Non-hydrogen atoms were refined to  $F^2$  anisotropically while hydrogen atoms were placed in calculated positions and isotropically refined assuming a "ride-on" model. The SHELX-97<sup>14</sup> program package was used for the structure determination, structure refinement, and tables. The drawings were made using the XP program of Bruker SHELXTL V5.1 program package.<sup>15</sup> Final unit cell parameters were obtained from a least-squares fit to the angular coordinates of all reflections. Crystal structure data have been deposited at the Cambridge Crystallographic Data Centre as supplementary publication Nos. CCDC 193256 (**1**· $\text{CH}_3\text{CN}$ ), CCDC 219201 (**2**), and CCDC 219200 (**4**). Enquires for data can be directed to CCDC, 12 Union Rd., Cambridge CB2 1EZ, U.K., or (E-mail) deposit@ccdc.cam.ac.uk.

### Computational Methods

The quantum chemical calculations were performed using Gaussian 98 program package.<sup>16</sup> The geometries of the isolated cations  $[(\text{DMAP})_2\text{PO}_2]^+$  ( $C_{2v}$  symmetry) and  $[(\text{DMAP})\text{POCl}_2]^+$  ( $C_s$ ) and the neutral molecule  $(\text{DMAP})\text{PO}_2\text{Cl}$  ( $C_s$ ) were calculated by density functional theory (DFT) and optimized at the B3LYP level<sup>17</sup> using polarized 6-31G(d,p) basis set.<sup>18</sup> The natural atomic charges<sup>19</sup> were calculated at the B3LYP/6-31G(d,p) level using the NBO analysis. The  $^{31}\text{P}$  nuclear shieldings were calculated by SOS-DFPT method at the PW91/IGLO-III level using deMon-KS program.<sup>20</sup> Theoretical  $^{31}\text{P}$  nuclear shieldings were converted to chemical shifts by the  $\delta = 328.35 - \sigma_{\text{theor}}$  relation, where the reference is the absolute shielding scale for  $^{31}\text{P}$ .<sup>21</sup>

### Results and Discussion

**Reactions of  $\text{POCl}_3$  with Pyridine and DMAP.** This study has confirmed the previously reported<sup>3</sup> inertness of dry pyridine toward  $\text{POCl}_3$ , if the latter was thoroughly purified from its hydrolysis products,  $\text{HCl}$  and  $\text{HPO}_2\text{Cl}_2$ . On the other hand, DMAP, as a stronger Lewis base,<sup>22</sup> reacts readily with  $\text{POCl}_3$  in acetonitrile solution and a white solid precipitates immediately. The isolated product is only

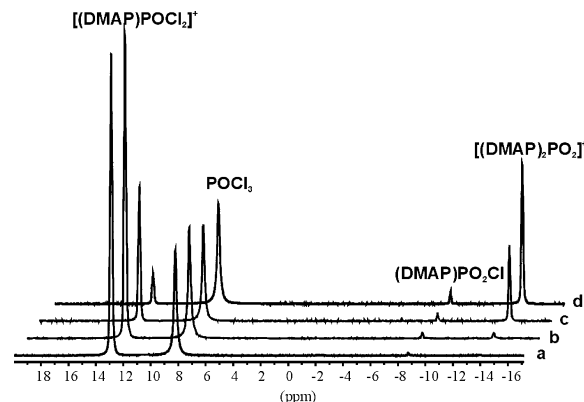


**Figure 1.** Time-dependent  $^{31}\text{P}$  NMR spectra of a reaction mixture with the molar ratio  $\text{DMAP}:\text{POCl}_3 = 1:1.4$  in  $\text{SO}_2$  solution: (a) 5 min; (b) 2 h; (c) 2 days; (d) 8 days.

sparingly soluble in acetonitrile but well soluble in the liquid sulfur dioxide. Its  $^{31}\text{P}$  NMR spectrum in  $\text{SO}_2$  solution consists of four singlets between 13.0 and  $-13.7$  ppm, suggesting the presence of a mixture of compounds.

When  $\text{POCl}_3$  was treated with DMAP directly in liquid  $\text{SO}_2$ , the reaction proceeded at a much slower rate, and after several days colorless crystals grew from the solution. The  $^{31}\text{P}$  NMR spectrum of their solution in  $\text{SO}_2$  showed a singlet at  $-13.6$  ppm, thus indicating that only a single phosphorus compound was formed.

Its X-ray single-crystal structure determination surprisingly revealed an ionic structure of the bis(4-(dimethylamino)pyridine)dioxophosphonium chloride, solvated by sulfur dioxide (**1**· $3\text{SO}_2$ ). Owing to a slight disorder in the  $\text{SO}_2$  molecules, however, only imperfect structural data ( $R_1 = 0.1082$ ) could be obtained. Recrystallization of **1**· $3\text{SO}_2$  from hot acetonitrile led to  $\text{SO}_2$  displacement, and an X-ray diffraction study of the obtained product revealed the structure of an acetonitrile solvate **1**· $\text{CH}_3\text{CN}$  with a fully acceptable value of  $R_1$  (0.0302).

The course of the reaction between DMAP and  $\text{POCl}_3$  in a  $\text{SO}_2$  solution was followed by monitoring the time dependence of relative intensities of the  $^{31}\text{P}$  NMR signals (Figure 1). The signals at  $-13.7$ ,  $-8.7$ , and  $8.3$  ppm can be assigned to **1**,  $(\text{DMAP})\text{PO}_2\text{Cl}$ ,<sup>23</sup> and  $\text{POCl}_3$ , respectively. The gradually disappearing peak at  $13.0$  ppm was assigned to the  $[(\text{DMAP})\text{POCl}_2]^+$  ion, which has been presumed earlier to exist in the binary  $\text{POCl}_3$ –pyridine system on the basis of conductivity measurements.<sup>4</sup> This assignment was supported by the calculation of isotropic  $^{31}\text{P}$  chemical shifts for the  $[(\text{DMAP})\text{POCl}_2]^+$ ,  $[(\text{DMAP})_2\text{PO}_2]^+$ , and  $[(\text{py})_2\text{PO}_2]^+$  ions and the previously reported adduct  $(\text{DMAP})\text{PO}_2\text{Cl}$ .<sup>23</sup> The results are presented and compared with the observed values in Table 4. Shift differences found for the already reported compounds  $(\text{DMAP})\text{PO}_2\text{Cl}$  and  $[(\text{DMAP})_2\text{PO}_2]\text{Cl}$  are lower than 6 ppm. Such a good agreement of calculated shifts with the experimental ones strongly supports our NMR identification of the  $[(\text{DMAP})\text{POCl}_2]^+$  cation.

On the basis of this assignment and the gradual changes in signal intensities, we have proposed a likely reaction

- (14) Sheldrick, G. M. *SHELX-97. Program for Crystal Structure Determination*; University of Göttingen: Göttingen, Germany, 1997.
- (15) Sheldrick, G. M. *SHELXTL V 5.1*; Bruker AXS Inc.: Madison, WI, 1998.
- (16) Frisch, M. J.; Trucks, G. W.; Schlegel, H. B.; Scuseria, G. E.; Robb, M. A.; Cheeseman, J. R.; Zakrzewski, V. G.; Montgomery, J. A., Jr.; Stratmann, R. E.; Burant, J. C.; Dapprich, S.; Millam, J. M.; Daniels, A. D.; Kudin, K. N.; Strain, M. C.; Farkas, O.; Tomasi, J.; Barone, V.; Cossi, M.; Cammi, R.; Mennucci, B.; Pomelli, C.; Adamo, C.; Clifford, S.; Ochterski, J.; Petersson, G. A.; Ayala, P. Y.; Cui, Q.; Morokuma, K.; Malick, D. K.; Rabuck, A. D.; Raghavachari, K.; Foresman, J. B.; Cioslowski, J.; Ortiz, J. V.; Baboul, A. G.; Stefanov, B. B.; Liu, G.; Liashenko, A.; Piskorz, P.; Komaromi, I.; Gomperts, R.; Martin, R. L.; Fox, D. J.; Keith, T.; Al-Laham, M. A.; Peng, C. Y.; Nanayakkara, A.; Gonzalez, C.; Challacombe, M.; Gill, P. M. W.; Johnson, B. G.; Chen, W.; Wong, M. W.; Andres, J. L.; Head-Gordon, M.; Replogle, E. S.; Pople, J. A. *Gaussian 98*, revision A.7; Gaussian, Inc.: Pittsburgh, PA, 1998.
- (17) Lee, C.; Yang, W.; Parr, R. G. *Phys. Rev.* **1988**, *B37*, 785.
- (18) Hehre, W. J.; Radom, L.; Schleyer, P. v. R.; Pople, J. A. *Ab Initio Molecular Theory*; Wiley: New York, 1986.
- (19) Reed, A. E.; Curtiss, L. A.; Weinhold, F. *Chem. Rev.* **1988**, *88*, 899.
- (20) Malkin, V. G.; Malkina, O. L.; Casida, M. E.; Salahub, D. R. *J. Am. Chem. Soc.* **1994**, *116*, 5898.
- (21) Jameson, C. J.; de Dios, A. C.; Jameson, A. K. *Chem. Phys. Lett.* **1990**, *167*, 575.
- (22) Maria, P.-C.; Gal, J.-F. *J. Phys. Chem.* **1985**, *89*, 1296.

- (23) Teichmann, H.; Schulz, J.; Costisella, B.; Habisch, D. Z. *Anorg. Allg. Chem.* **1991**, *606*, 233.

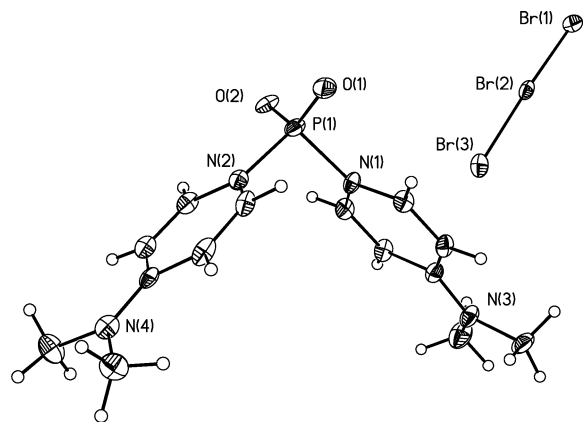
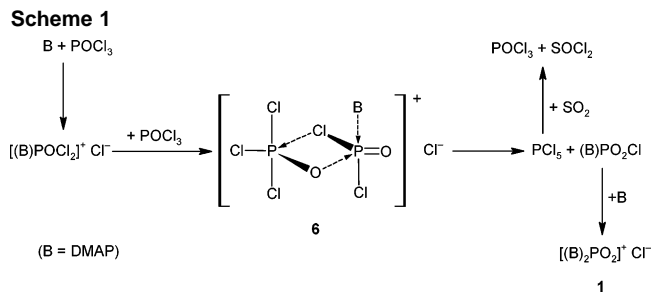


**Figure 2.** ORTEP representation of  $[(\text{DMAP})_2\text{PO}_2]^+\text{Br}_3^-$  (**2**) with 50% probability ellipsoids.

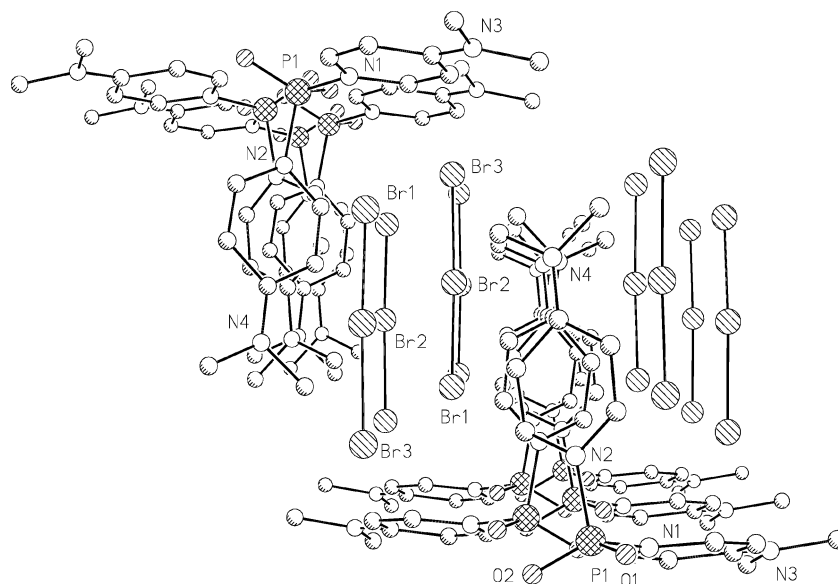
pathway involving all observed species (Scheme 1). In the initial step, a base-induced ionization of  $\text{POCl}_3$  proceeds under heterolytic cleavage of one P–Cl bond and the simultaneous formation of the ion  $[(\text{DMAP})\text{POCl}_2]^+$ . Its successive reaction with  $\text{POCl}_3$  gives presumably an intermediate, oxygen- and chlorine-bridged binuclear cation **6**. This cation then undergoes a nucleophilic attack by  $\text{Cl}^-$  ion and decomposes into betaine  $(\text{DMAP})\text{PO}_2\text{Cl}$  and  $\text{PCl}_5$ . Subsequent displacement of the  $\text{Cl}^-$  ion from  $(\text{DMAP})\text{PO}_2\text{Cl}$  by the more basic DMAP yields **1** as the final product. No NMR signals of the formed phosphorus pentachloride, either in its molecular or ionically dissociated  $[\text{PCl}_4]^+$  and  $[\text{PCl}_6]^-$  forms, were detected due to its subsequent reaction with  $\text{SO}_2$ , which yielded equimolar amounts of  $\text{POCl}_3$  and  $\text{SOCl}_2$ .<sup>24</sup> The formation of the latter was proved by Raman spectroscopy: the frequencies observed at 1231 ( $\nu(\text{SO})$ ), 487 ( $\nu_s(\text{SCl})$ ), 444 ( $\nu_{as}(\text{SCl})$ ), and 343 ( $\delta_s(\text{SCl}_2)$ )  $\text{cm}^{-1}$  agree well with literature values reported for the fundamental modes of thionyl chloride.<sup>25</sup>



**Reactions of  $\text{POBr}_3$  with Pyridine and DMAP.** In contrast to  $\text{POCl}_3$ , phosphorus oxide bromide reacts smoothly with both DMAP and pyridine to give crystalline products **2** and **3**, respectively. Because **2** obtained in this way is often contaminated by intermediates sparingly soluble in acetonitrile, its preparation by the transamination of **3** with DMAP appears to be more reliable route. The molecular structure of **2** (Figure 2) was determined by X-ray crystal analysis. However, any attempts to grow suitable crystals of **3** have failed. For this reason, the tribromide **3** has been converted into a triflate **4**, whose well-formed crystals allowed its crystal structure determination (Figure 3) without difficulties.

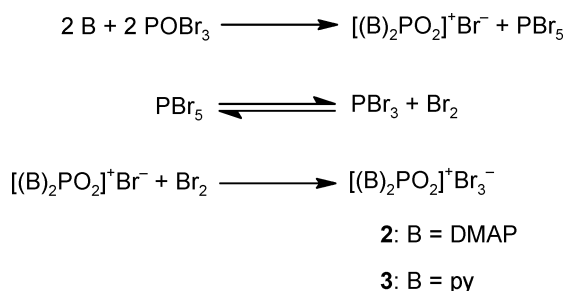
In both cases, the reaction course is similar to that of the base-induced dismutation of  $\text{POCl}_3$ . The apparent difference is that  $\text{PBr}_5$ , formed in the reaction, decomposes to elemental bromine and  $\text{PBr}_3$ , whose formation was confirmed by  $^{31}\text{P}$  NMR spectroscopy (s, 230.6 ppm). The liberated  $\text{Br}_2$  molecule adds readily on the bromide anion to give  $\text{Br}_3^-$ . In acetonitrile the resulting tribromides **2** and **3** are less soluble and crystallize from the reaction solution.

The other signals observed at  $-33.5$  and  $-24.7$  ppm can be assigned to the donor-stabilized cations  $[(\text{DMAP})\text{POBr}_2]^+$  and  $[(\text{py})\text{POBr}_2]^+$ , respectively. In contrast to the betaines  $(\text{DMAP})\text{PO}_2\text{Cl}$  and  $(\text{py})\text{PO}_2\text{Cl}$ , however, their bromine analogues are probably highly susceptible to a nucleophilic attack of another base molecule and convert easily into the corresponding donor-stabilized cations  $[(\text{DMAP})_2\text{PO}_2]^+$  or



**Figure 3.** Packing of  $[(\text{DMAP})_2\text{PO}_2]^+$  and  $\text{Br}_3^-$  in the crystal structure of **2** viewed along the  $b$ -axis. Hydrogen atoms are omitted for clarity.

## Scheme 2

**Table 1.** Crystal and Structure Refinement Data for **1**·CH<sub>3</sub>CN, **2**, and **4**

	<b>1</b> ·CH <sub>3</sub> CN	<b>2</b>	<b>4</b>
chem formula	C <sub>16</sub> H <sub>23</sub> ClN <sub>5</sub> O <sub>2</sub> P	C <sub>14</sub> H <sub>20</sub> Br <sub>3</sub> N <sub>4</sub> O <sub>2</sub> P	C <sub>13</sub> H <sub>13</sub> F <sub>3</sub> N <sub>5</sub> O <sub>5</sub> PS
fw	383.81	547.04	411.29
temp (K)	120	120	120
space group	<i>P</i> $\bar{1}$	<i>P</i> 2 <sub>1</sub> / <i>c</i>	<i>P</i> 2 <sub>1</sub> / <i>n</i>
<i>a</i> (Å)	8.910(2)	13.406(3)	12.550(3)
<i>b</i> (Å)	10.128(2)	12.932(3)	8.810(2)
<i>c</i> (Å)	10.282(2)	11.024(2)	15.357(3)
$\alpha$ (deg)	89.47(3)	90	90
$\beta$ (deg)	82.93(3)	93.77(3)	93.95(3)
$\gamma$ (deg)	89.03(3)	90	90
<i>V</i> (Å <sup>3</sup> )	920.6(3)	1907.1(7)	1693.9(6)
<i>Z</i>	2	4	4
$\mu$ (mm <sup>-1</sup> )	0.315	6.445	0.348
<i>D</i> (Mg/m <sup>3</sup> )	1.385	1.905	1.613
R-indices [ <i>I</i> > 2 $\sigma$ ( <i>I</i> )]	R1 <sup>a</sup> = 0.0302	R1 <sup>a</sup> = 0.0525	R1 <sup>a</sup> = 0.0395
R-indices (all data)	R1 = 0.0374	R1 = 0.0830	R1 = 0.0630

$$^a \text{R1} = \sum |F_o| - |F_c| / \sum |F_o|.$$

**Table 2.** Selected Bond Lengths (Å) and Angles (deg) for **1**·CH<sub>3</sub>CN and **2** and Calculated Parameters of [(DMAP)<sub>2</sub>PO<sub>2</sub>]<sup>+</sup>

	<b>1</b> ·CH <sub>3</sub> CN	<b>2</b>	calcd (B3LYP/6-31G(d,p))
P–O(1)	1.4671(11)	1.460(4)	1.48
P–O(2)	1.4626(12)	1.465(4)	1.48
P–N(1)	1.7653(12)	1.748(4)	1.83
P–N(2)	1.7476(12)	1.728(4)	1.83
C(arom)–N(arom) <sup>a</sup>	1.3666(18)	1.367(6)	1.36
C(arom)–C(arom) <sup>a</sup>	1.3892(19)	1.381(7)	1.40
Br(1)–Br(2)		2.4842(10)	
Br(2)–Br(3)		2.6015(10)	
O(1)–P–O(2)	127.11(7)	126.8(2)	134.7
O(1)–P–N(1)	105.45(6)	106.7(2)	104.4
O(1)–P–N(2)	107.07(6)	107.6(2)	104.4
O(2)–P–N(1)	107.53(6)	105.7(2)	104.4
O(2)–P–N(2)	106.3(7)	107.4(2)	104.4
N(1)–P–N(2)	100.66(6)	99.4(2)	99.6
Br(1)–Br(2)–Br(3)		177.77(3)	

<sup>a</sup> Average bond lengths.

[(py)<sub>2</sub>PO<sub>2</sub>]<sup>+</sup>. For this reason, the <sup>31</sup>P NMR signals of anticipated betaines, (DMAP)PO<sub>2</sub>Br and (py)PO<sub>2</sub>Br, have not been observed. The likely pathway of these reactions is shown in Scheme 2.

**Crystal Structures of [(DMAP)<sub>2</sub>PO<sub>2</sub>]Cl·CH<sub>3</sub>CN (**1**·CH<sub>3</sub>CN) and [(DMAP)<sub>2</sub>PO<sub>2</sub>][Br<sub>3</sub>] (**2**).** Crystallographic data for **1**·CH<sub>3</sub>CN and **2** are summarized in Table 1. Selected bond lengths and angles for **1**·CH<sub>3</sub>CN and **2**, together with the calculated bond parameters of the [(DMAP)<sub>2</sub>PO<sub>2</sub>]<sup>+</sup> cation, are listed in Table 2. The phosphorus atom in the [(DMAP)<sub>2</sub>PO<sub>2</sub>]<sup>+</sup> ion exhibits in **1**·CH<sub>3</sub>CN and **2** (Figure 2) a strongly distorted tetrahedral coordination with bond angles ranging from 99.4 to 127.1°. The reported quantum-chemical

calculations showed an increasing value of the O–P–O bond angle in the series [PO<sub>2</sub>]<sup>−</sup> anion (119.5°),<sup>26</sup> [PO<sub>2</sub>]<sup>•</sup> radical (136.8°),<sup>27</sup> and the linear [PO<sub>2</sub>]<sup>+</sup> cation. The approximately 127° O–P–O angle in **1**·CH<sub>3</sub>CN and **2** thus illustrates a change in the [PO<sub>2</sub>]<sup>+</sup> geometry caused by coordination of two DMAP molecules. However, the average P–O bond distance of 1.464 Å in **1**·CH<sub>3</sub>CN and **2** is only slightly longer than the value of 1.450 Å calculated for the hypothetical [PO<sub>2</sub>]<sup>+</sup> ion at the B3LYP/6-31G(d,p) level and indicates a considerable multiple P–O bond order sustaining in [(DMAP)<sub>2</sub>PO<sub>2</sub>]<sup>+</sup>. Nearly equal P–O bond length of 1.457 Å in [PO<sub>2</sub>F<sub>2</sub>]<sup>−</sup><sup>28</sup> suggests a comparable  $\pi$ -character of the P–O bonds in both ions. The high electronegativity of F-ligands apparently fully compensates the negative charge of the [PO<sub>2</sub>F<sub>2</sub>]<sup>−</sup> ion. The average P–N bond lengths of 1.756 Å (**1**·CH<sub>3</sub>CN) and 1.738 Å (**2**) are somewhat longer than the single P–N bond in [PO<sub>2</sub>(NH<sub>2</sub>)<sub>2</sub>]<sup>−</sup> (1.678 Å)<sup>29</sup> but significantly shorter than a typical P–N dative bond in the betaine (py)PS<sub>2</sub>Cl (1.849 Å).<sup>30</sup> This shortening can be attributed to a greater Lewis acidity of [PO<sub>2</sub>]<sup>+</sup> with respect to the PS<sub>2</sub>Cl molecule and in part to the overall positive charge of [(DMAP)<sub>2</sub>PO<sub>2</sub>]<sup>+</sup>.

Pyridine rings in the [(DMAP)<sub>2</sub>PO<sub>2</sub>]<sup>+</sup> ion are virtually planar and with torsion angles 91.3 and 83.3° roughly orthogonal to the N(1)–P(1)–N(2) plane in **2**, while in **1**·CH<sub>3</sub>CN two unequal torsion angles 52.7 and 80.1° have been observed. The geometry of the amine nitrogen is essentially also planar, indicating a considerable conjugation between the lone pair of the amine nitrogen and the  $\pi$ -system of the pyridine ring. Such a conjugation leads to a partly quinoidal character<sup>31</sup> of the pyridinium system and, consequently, to a shortening of the ring bond distances C(1)–C(2) and C(4)–C(5) and in exocyclic N(3)–C(3) and N(4)–C(10) bonds. With respect to the neat crystalline DMAP,<sup>32</sup> the two former bonds in **2** are shorter by 0.03 Å, while the latter two are shortened by 0.05 Å. Similarly, as in crystalline DMAP, the dimethylamino group in **1**·CH<sub>3</sub>CN and **2** is slightly twisted from the pyridine ring plane and the corresponding torsion angle varies between 4.7 and 5.3° in both structures.

Each [(DMAP)<sub>2</sub>PO<sub>2</sub>]<sup>+</sup> ion in **2** exhibits two C–H⋯O contacts which occur between its oxygen atoms and the hydrogen atoms of the nearest pyridine ring in a neighboring cation. The observed H⋯O distances of 2.31 and 2.46 Å in C(2)–H(2)⋯O(2)<sup>i</sup> and C(1)–H(1)⋯O(1)<sup>i</sup> hydrogen bridges (symmetry codes (i): +*x*, 1/2 + *y*, 1/2 + *z*) are only moderately shorter than the sum of the van der Waals radii (2.74 Å). However, these weak C–H⋯O interactions result in the formation of infinite cation chains with a half of their

(24) Becke-Goehring, M.; Lehr, W. *Chem. Ber.* **1961**, *94*, 1591.

(25) Gillespie, R. J.; Robinson, E. A. *Can. J. Chem.* **1961**, *39*, 2171.

(26) Xu, C.; de Beer, E.; Neumark, D. M. *J. Chem. Phys.* **1996**, *104*, 2749.

(27) Cai, Z. L.; Hirsch, G.; Beunker, R. *J. Chem. Phys. Lett.* **1996**, *255*, 350.

(28) Harrison, R. W.; Thompson, R. C.; Trotter, J. *J. Chem. Soc. A* **1966**, 1775.

(29) Jacobs, H.; Nymwegen, R. *Z. Anorg. Allg. Chem.* **1997**, *623*, 849.

(30) Averbuch-Pouchot, M. T.; Meisel, M. *Acta Crystallogr.* **1989**, *C45*, 1937.

(31) Kolomeitsev, A.; Schoth, R.-M.; Röschenhaler, G.-V. *Chem. Commun.* **1996**, 335.

(32) Ohms, U.; Guth, H. *Z. Kristallogr.* **1984**, *166*, 213.

**Table 3.** Selected Bond Lengths (Å) and Angles (deg) for **4**

P–O(1)	1.4576(15)	O(1)–P–O(2)	129.50(8)
P–O(2)	1.4585(14)	O(1)–P–N(1)	106.30(8)
P–N(1)	1.7825(17)	O(1)–P–N(2)	106.59(8)
P–N(2)	1.797(17)	O(2)–P–N(1)	107.28(8)
C(arom)–N(arom) <sup>a</sup>	1.354(2)	O(2)–P–N(2)	105.44(8)
C(arom)–C(arom) <sup>a</sup>	1.376(7)	N(1)–P–N(2)	97.10(8)

<sup>a</sup> Average bond lengths.

DMAP rings stacked approximately in the *ab* plane. The other half of the rings, lying parallel to the *bc* plane, occupies intermittently lateral positions along both sides of the *ac* plane. These chains form channels, each of which is occupied by two parallel rows of approximately collinear Br<sub>3</sub><sup>−</sup> anions (Figure 3). Anions in adjacent rows exhibit a reverse orientation.

The Br<sub>3</sub><sup>−</sup> in **2** is a discrete anion, and the shortest distance between the positively charged phosphorus in the [(DMAP)<sub>2</sub>PO<sub>2</sub>]<sup>+</sup> cation and the surrounding bromines is 7.304 Å, which confirms a predominant ionic character of the compound. With its moderately disparate bond lengths (2.484 and 2.601 Å) and a slight deviation from linearity (177.8°), the geometry of Br<sub>3</sub><sup>−</sup> is very close to that previously reported for [P(CH<sub>3</sub>)<sub>4</sub>][Br<sub>3</sub>].<sup>33</sup>

Two bromine atoms in each Br<sub>3</sub><sup>−</sup> ion have always one long anion–cation C–H⋯Br contact to the nearest pyridine molecule in the adjacent cation. Although the corresponding H⋯Br distances, 2.93 and 3.05 Å, are only slightly shorter than the sum of the van der Waals radii (3.07 Å), the formation of weak C–H⋯Br hydrogen bridges can be assumed. Their stability may be caused by an enhanced positive charge on the H atoms of the DMAP rings resulting from the formation of the dative N–P bond (Figure 5). The occurrence of similar C–H⋯Cl bridges was encountered in an ionic complex [SiH<sub>2</sub>(py)<sub>4</sub>]Cl<sub>2</sub>·4CHCl<sub>3</sub>.<sup>34</sup>

The separation between the adjacent DMAP ring layers lying in the *bc* plane is 5.27 Å, while in the *b* direction the inter-ring distances are even longer (6.01 Å). Both distances are too large, however, to enable a π–π stacking interactions of aromatic rings.

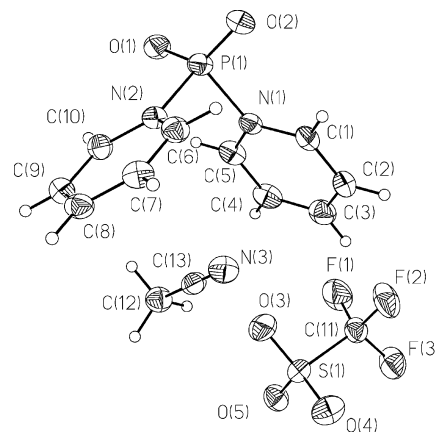
Despite the very similar structural parameters of [(DMAP)<sub>2</sub>PO<sub>2</sub>]<sup>+</sup> in **1**·CH<sub>3</sub>CN and **2**, the cations exhibit different intermolecular interactions in particular crystal structures. In contrast to **2**, neither the C–H⋯O nor the C–H⋯Cl intermolecular contacts involving the aromatic ring hydrogens have been observed in the crystal structure of **1**·CH<sub>3</sub>CN. Instead, only H⋯O interactions (2.538 Å) with hydrogens of the dimethylamino group and certain very long H⋯Cl contacts (2.978 Å) to the solvating acetonitrile have been found.

**Crystal Structure of [py<sub>2</sub>PO<sub>2</sub>][CF<sub>3</sub>SO<sub>3</sub>]<sup>−</sup>·CH<sub>3</sub>CN (**4**).** The crystal data for **4** are given in Table 1, and important bond lengths and angles for the [(py)<sub>2</sub>PO<sub>2</sub>]<sup>+</sup> cation are listed in Table 3. The crystal structure of **4** revealed that the coordination of [PO<sub>2</sub>]<sup>+</sup> by different N-donor molecules

**Table 4.** Calculated and Experimental Values of Chemical Shifts (ppm) for N-Donor Coordinated Molecules and Ions Observed in <sup>31</sup>P NMR Spectra

compd	δ <sub>calcd</sub>	δ <sub>expt</sub>	solvent
[(DMAP)POCl <sub>2</sub> ] <sup>+</sup> ( <b>I</b> )	24.3	13.0 <sup>b</sup>	SO <sub>2</sub>
[(DMAP)POCl <sub>2</sub> ] <sup>+</sup> ( <b>II</b> )	17.1	13.0 <sup>b</sup>	
(DMAP)PO <sub>2</sub> Cl	−3.1	−8.6 <sup>20</sup>	CH <sub>3</sub> NO <sub>2</sub>
		−8.7 <sup>b</sup>	SO <sub>2</sub>
[(DMAP) <sub>2</sub> PO <sub>2</sub> ] <sup>+</sup>	−15.4	−13.6 <sup>18,a</sup>	unknown
		−13.7 <sup>b</sup>	SO <sub>2</sub>
[(py) <sub>2</sub> PO <sub>2</sub> ] <sup>+</sup>	−13.3	−14.6 <sup>b</sup>	SO <sub>2</sub>

<sup>a</sup> [SbCl<sub>6</sub>]<sup>−</sup> salt. <sup>b</sup> This work.

**Figure 4.** ORTEP representation of [(py)<sub>2</sub>PO<sub>2</sub>]<sup>+</sup>[CF<sub>3</sub>SO<sub>3</sub>]<sup>−</sup>·CH<sub>3</sub>CN (**4**) with 50% probability ellipsoids.

apparently does not affect substantially the geometry of the resulting complex and that the cation [(py)<sub>2</sub>PO<sub>2</sub>]<sup>+</sup> (Figure 4) differs from [(DMAP)<sub>2</sub>PO<sub>2</sub>]<sup>+</sup> mainly in the P–N bond lengths. Their lengthening by 0.03 and 0.05 Å with respect to the [(DMAP)<sub>2</sub>PO<sub>2</sub>]<sup>+</sup> ion in **1**·CH<sub>3</sub>CN and **2**, respectively, is consistent with the decreased Lewis basicity of pyridine relative to DMAP.<sup>22</sup> A slight reduction of the N–P bond order is reflected also in the corresponding changes of bond angles. Consequently, the N–P–N angle in **4** is decreased by 2.3 or 3.6° with respect to the [(DMAP)<sub>2</sub>PO<sub>2</sub>]<sup>+</sup> in **2** or **1**·CH<sub>3</sub>CN, while a simultaneous widening of the O–P–O angle by 2.7 or 3.6° occurs. We have found nothing unusual in the crystal packing of **4**, and the [(py)<sub>2</sub>PO<sub>2</sub>]<sup>+</sup> cations are without any contact below the sum of the van der Waals radii. The only observed intermolecular C–H⋯O contacts (2.485 Å) occur between acetonitrile and an oxygen atom of the triflate anion.

**Comparison with Previous Reports on [(DMAP)<sub>2</sub>PO<sub>2</sub>]<sup>+</sup> and Related Cations.** The crystal structure analysis and <sup>31</sup>P NMR spectroscopy revealed that compounds **1**·3SO<sub>2</sub>, **1**·CH<sub>3</sub>CN, and **2**–**5** can all be considered as salts of the donor-stabilized [PO<sub>2</sub>]<sup>+</sup> ion, an unknown analogue of the nitronium ion, [NO<sub>2</sub>]<sup>+</sup>. Recently reported attempts to produce the [PO<sub>2</sub>]<sup>+</sup> ion by treatment of KPO<sub>2</sub>F<sub>2</sub> with excess SbF<sub>5</sub> failed to provide [PO<sub>2</sub>]<sup>+</sup>[SbF<sub>6</sub>]<sup>−</sup>, and an eight-membered oxygen-bridged heterocycle, (SbF<sub>4</sub>O<sub>2</sub>PF<sub>2</sub>)<sub>2</sub>, was obtained instead.<sup>35</sup> The ligand-stabilized cation, [(DMAP)<sub>2</sub>PO<sub>2</sub>]<sup>+</sup>, was previously prepared as triflate by a rather complex reaction between

(33) Robertson, K. N.; Bakshi, P. K.; Cameron, T. S.; Knop, O. Z. *Anorg. Allg. Chem.* **1997**, *623*, 104.

(34) Hensen, K.; Stumpf, T.; Bolte, M.; Näther, C.; Fleischer, H. J. *Am. Chem. Soc.* **1998**, *120*, 10402.

(35) Schneider, S.; Vij, A.; Sheehy, J. A.; Tham, F. S.; Schroer, T.; Christie, K. O. Z. *Anorg. Allg. Chem.* **2001**, *627*, 631.

CH<sub>3</sub>OP(O)Cl<sub>2</sub>, DMAP, and trimethylsilyl triflate.<sup>36</sup> The isolated precipitate was briefly characterized by IR, <sup>1</sup>H, and <sup>31</sup>P NMR spectra. However, the reported chemical shift at -19.08 ppm in CD<sub>3</sub>NO<sub>2</sub> appears about 5 ppm upfield from the values obtained in the present work, although our results suggest that the <sup>31</sup>P chemical shift of [(DMAP)<sub>2</sub>PO<sub>2</sub>]<sup>+</sup> is neither solvent-dependent nor affected by its counterion. Later, the formation of [(DMAP)<sub>2</sub>PO<sub>2</sub>]<sup>+</sup> and [(DMAP)<sub>2</sub>POS]<sup>+</sup> obtained upon treatment of the betaines (DMAP)PO<sub>2</sub>Cl and (DMAP)PO<sub>2</sub>OSi, respectively, with excess DMAP was briefly mentioned.<sup>37</sup> The crystalline salts were isolated as chlorides, tetraphenylborates, triflates, and hexachloroantimonates, but no experimental details were given, except for melting points and <sup>31</sup>P chemical shifts. Although the used solvent was not specified, the reported chemical shifts between -13.6 and -14.2 ppm are in excellent agreement with our results. Similar donor-stabilized ions, [(py)<sub>2</sub>PS<sub>2</sub>]<sup>+</sup><sup>38</sup> and [(DMAP)<sub>2</sub>P(=NR)<sub>2</sub>]<sup>+</sup>,<sup>39</sup> were described recently. Together with [(py)<sub>2</sub>PO<sub>2</sub>]<sup>+</sup>, [(DMAP)<sub>2</sub>PO<sub>2</sub>]<sup>+</sup>, and [(DMAP)<sub>2</sub>POS]<sup>+</sup>, they constitute an interesting series of bis(donor)-stabilized bis(chalcogeno/imino)phosphonium cations.

**Quantum Chemical Calculations.** A comparison of experimental and ab initio optimized structural parameters of the PO<sub>2</sub>N<sub>2</sub> moiety in [(DMAP)<sub>2</sub>PO<sub>2</sub>]<sup>+</sup> ion (Table 2) shows a good agreement of almost all bond angles and P-O bond lengths, except for the calculated P-N bond length, which is longer by 0.074 or 0.092 Å than that found in crystalline **1**·CH<sub>3</sub>CN or **2**. It should be taken into account, however, that the bond parameters were calculated for an isolated ion and need not be well comparable with the results of X-ray diffraction. Significant bond length differences between the gas phase and the solid state are indeed often encountered in complexes with dative bonds.<sup>40</sup>

The calculated bond lengths C(1)-C(2), C(4)-C(5), and C(3)-N(3) within the DMAP moiety in the [(DMAP)<sub>2</sub>PO<sub>2</sub>]<sup>+</sup> ion are, relative to DMAP itself, shorter by 0.021, 0.021, and 0.032 Å, respectively. This slight shortening is in accordance with the predicted quinoidal character of the donor DMAP molecule and has been revealed by X-ray structure analysis.

The distribution of natural atomic charges in the noncoordinated [PO<sub>2</sub>]<sup>+</sup>, DMAP, and the [(DMAP)<sub>2</sub>PO<sub>2</sub>]<sup>+</sup> cation is shown in Figure 5. The total amount of charge transfer from both DMAP molecules to the [PO<sub>2</sub>]<sup>+</sup> ion is 0.72 e and results in an extensive delocalization of its intrinsic positive charge. This calculated value is roughly comparable with the charge transfer of 0.54 and 0.58 electrons obtained experimentally for the gas-phase adducts (C<sub>5</sub>H<sub>5</sub>N)SO<sub>3</sub><sup>41</sup> and (Me<sub>3</sub>N)SO<sub>3</sub>,<sup>42</sup> respectively, where the SO<sub>3</sub> is also a strong

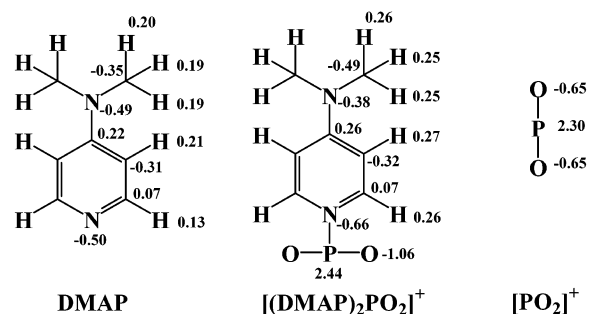


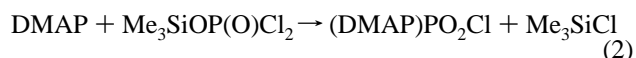
**Figure 5.** Distribution of natural atomic charges in DMAP, [PO<sub>2</sub>]<sup>+</sup>, and [(DMAP)<sub>2</sub>PO<sub>2</sub>]<sup>+</sup>.

Lewis acid. In comparison with the [PO<sub>2</sub>]<sup>+</sup> ion and DMAP, the phosphorus and hydrogen atoms in [(DMAP)<sub>2</sub>PO<sub>2</sub>]<sup>+</sup> become more positive, while the oxygen and donor nitrogen atoms more negative, indicating a contribution of electrostatic attraction to the formation of the N-P donor-acceptor bonds. In addition, an enhanced positive charge on the pyridine ring hydrogen atoms creates a precondition for the formation of intermolecular C-H...O and C-H...Br bridges, which have indeed been found in the crystal structure of **2**.

During the optimization of the [(DMAP)POCl<sub>2</sub>]<sup>+</sup> ion geometry, two stationary points were obtained. The first one (**I**), with the DMAP ring lying in the O-P-N plane, has been characterized as being a true minimum on the potential energy surface. The conformer **II**, in which the plane of DMAP ring is perpendicular to the O-P-N plane, has been characterized as first-order saddle point (one imaginary vibrational frequency revealed by the frequency analysis) and represents a transition state for the DMAP rotation around the N-P bond. The energy difference between **I** and **II** is 4.46 kcal mol<sup>-1</sup>.

**Reactions of **1**·CH<sub>3</sub>CN and **3** with Trimethylsilyl Phosphorodihalidates and Trifluoromethanesulfonate.** The dihalogenophosphates [(DMAP)<sub>2</sub>PO<sub>2</sub>][PO<sub>2</sub>X<sub>2</sub>] (X = F, Cl) can be considered ionic dimers of molecular betaines (DMAP)PO<sub>2</sub>X, and we have attempted their synthesis from **1**·CH<sub>3</sub>CN by appropriate anion exchange reactions. The readily accessible trimethylsilyl phosphorodifluoridate and phosphorodichloridate, which give with Cl<sup>-</sup> the volatile Me<sub>3</sub>-SiCl as the leaving group, have been chosen as suitable sources of dihalogenophosphate groups. However, a different course of reactions between **1**·CH<sub>3</sub>CN and the two esters has been observed.

Although the [(DMAP)<sub>2</sub>PO<sub>2</sub>]<sup>+</sup> ion exhibits a considerable stability even in aqueous solution, an equilibrium between the cation, free DMAP, and the neutral betaine, (DMAP)PO<sub>2</sub>Cl, is established on heating in CH<sub>3</sub>CN solution. When the stoichiometric amount of Me<sub>3</sub>SiOP(O)Cl<sub>2</sub> is then added, it is partly consumed in a side reaction with the released DMAP under formation of another betaine molecule.<sup>43</sup>



Thus, in addition to [(DMAP)<sub>2</sub>PO<sub>2</sub>][PO<sub>2</sub>Cl<sub>2</sub>], (DMAP)PO<sub>2</sub>-Cl and other byproducts are formed as well.

(36) Weiss, R.; Engel, S. *Angew. Chem.* **1992**, *104*, 239; *Angew. Chem., Int. Ed. Engl.* **1992**, *31*, 216.

(37) Teichmann, H. *Phosphorus, Sulfur, Silicon* **1993**, *76*, 355/95.

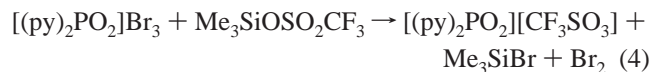
(38) Meisel, M.; Lönnecke, P.; Grimmer, A.-R.; Wulff-Molder, D. *Angew. Chem.* **1997**, *109*, 1940; *Angew. Chem., Int. Ed. Engl.* **1997**, *36*, 1869.

(39) Blättner, M.; Nieger, M.; Ruban, A.; Schoeller, W. W.; Niecke, E. *Angew. Chem.* **2000**, *112*, 2876; *Angew. Chem., Int. Ed.* **2000**, *39*, 2768.

(40) Leopold, K. R.; Canagaratna, M.; Phillips, J. A. *Acc. Chem. Res.* **1997**, *30*, 57 and references therein.

(41) Hunt, S. W.; Leopold, K. R. *J. Phys. Chem.* **2001**, *105A*, 5498.

On the other hand, if a solution of  $\mathbf{1}\cdot\text{CH}_3\text{CN}$  is heated with  $\text{Me}_3\text{SiOP}(\text{O})\text{F}_2$ , anion exchange occurs and, according to the  $^{31}\text{P}$  NMR spectroscopy, only pure  $\mathbf{5}$  is formed. Instead of  $\mathbf{1}\cdot\text{CH}_3\text{CN}$ , the tribromide  $\mathbf{3}$  can also be used, and treatment of its acetonitrile solution with  $\text{Me}_3\text{SiOSO}_2\text{CF}_3$  yields the corresponding triflate  $\mathbf{4}$ .



## Conclusions

Previously only briefly described  $[(\text{DMAP})_2\text{PO}_2]^+$ <sup>36,37</sup> and the new  $[(\text{py})_2\text{PO}_2]^+$  cations have been synthesized as chlorides and tribromides by the treatment of phosphoryl chloride or bromide with pyridine bases. The formation of previously reported adducts<sup>4–6</sup> in these reactions was not confirmed, and their existence seems to be doubtful. According to the results obtained, the  $\text{POCl}_3$  reacts only with DMAP, the strongest simple Lewis base,<sup>22</sup> under heterolytic cleavage of one P–Cl bond in the first stage. In contrast to the neutral, mononuclear *trans*- $\text{SiCl}_4(\text{py})_2$ ,<sup>8</sup> no covalent  $\text{POCl}_3$  complex with hexacoordinated P-atom is formed, probably due to a steric hindrance against increasing of the coordination number exerted by the P=O double bond. With the exception of presumed intermediate  $\mathbf{6}$ , the tetracoordinated P-atom is maintained in all species involved in the

(42) Fiacco, D. L.; Toro, A.; Leopold, K. R. *Inorg. Chem.* **2000**, *39*, 37.

(43) Cerník, M. To be published.

subsequent reaction steps. The formation of a cation  $[\text{P}(\text{O})\text{Cl}(\text{L})_4]^{2+}$  (L = Lewis base), analogous to the reported  $[\text{SiCl}_2(\text{NMI})_4]^{2+}$ ,<sup>9</sup> is thus hindered, and a base-catalyzed dismutation of  $\text{POCl}_3$  to  $\text{PCl}_5$  and  $\text{ClPO}_2$  occurs. The coordinatively unsaturated  $\sigma^3$ - $\lambda^5$ -phosphorane  $\text{ClPO}_2$ <sup>44</sup> is ligand-stabilized as the adduct  $(\text{DMAP})\text{PO}_2\text{Cl}$ , which is then transformed into the  $[(\text{DMAP})_2\text{PO}_2]^+$  cation in its subsequent reaction with another DMAP molecule. The reactions of  $\text{POBr}_3$  with pyridines proceed analogously, but besides DMAP also the pyridine exhibits a sufficient Lewis basicity to initiate the dismutation process. From a mechanistic point of view, the observed base-induced dismutation of  $\text{POCl}_3$  and  $\text{POBr}_3$  closely resembles the pathway suggested recently for the  $\text{F}^-$ -catalyzed dismutation of  $\text{POF}_3$ .<sup>45</sup> The elucidation of these and other similar halogen/oxygen exchanges in halogenide oxides of pnictogens is, therefore, of particular interest and should attract further attention.

**Acknowledgment.** This work was supported by the Ministry of Education of the Czech Republic (Grants MSM 143100011 and MSM 100000001). L.K. is grateful to the Brno Supercomputing Center for the computing time.

**Supporting Information Available:** Crystallographic data in CIF format for complexes  $\mathbf{1}\cdot\text{CH}_3\text{CN}$ ,  $\mathbf{2}$ , and  $\mathbf{4}$  and calculated Cartesian coordinates for  $[(\text{DMAP})\text{POCl}_2]^+$  and  $[(\text{DMAP})_2\text{PO}_2]^+$  ions and betaine  $(\text{DMAP})\text{PO}_2\text{Cl}$ . This material is available free of charge via the Internet at <http://pubs.acs.org>.

IC0354163

(44) Meisel, M.; Bock, H.; Solouki, B.; Kremer, M. *Angew. Chem.* **1989**, *101*, 1378; *Angew. Chem., Int. Ed. Engl.* **1989**, *28*, 1373.

(45) Christe, K. O.; Dixon, D. A.; Schrobilgen, G. J.; Wilson, W. W. *J. Am. Chem. Soc.* **1997**, *119*, 3918.